Open Access

Catalysis Research

LIDSEN Publishing Inc.

Original Research

Heterologous Expression, Characterization, and Comparison of Laccases from the White Rot Causing Basidiomycete Cerrena Unicolor

Le Thanh Mai Pham [1, 2], Kai Deng [1, 2], Trent R. Northen [1, 3], Steven W. Singer [1, 3], Paul D. Adams [1, 3, 4], Blake A. Simmons [1, 3], Kenneth L. Sale [1, 2, *]

1. Joint BioEnergy Institute, Emeryville, CA 94608, USA; E-Mails: thanhmaipl@lbl.gov; kdeng@lbl.gov; trnorthen@lbl.gov; swsinger@lbl.gov; pdadams@lbl.gov; basimmons@lbl.gov; klsale@sandia.gov; klsale@lbl.gov
2. Sandia National Laboratories, Livermore, CA, 94550, USA
3. Lawrence Berkeley National Laboratory, Berkeley, CA 94720, USA
4. University of California, Berkeley, CA 94720, USA

* **Correspondence:** Kenneth L. Sale; E-Mails: klsale@sandia.gov; klsale@lbl.gov

Academic Editor: Robert Wojcieszak

Special Issue: Recent Advances in Catalysis for Biomass Conversion

Catalysis Research
2022, volume 2, issue 3
doi:10.21926/cr.2203028

Received: July 26, 2022
Accepted: September 14, 2022
Published: September 20, 2022

Abstract

Lignin is the most abundant renewable source of aromatics on earth, and conversion of it to chemicals and fuels is needed to build an economically viable renewable biofuels industry. Biological routes to converting lignin to fuels and chemicals involve depolymerizing lignin using lignin-degrading enzymes that catalyze the breaking of ether and carbon-carbon bonds in the phenolic and non-phenolic subunits of lignin. Laccases are a crucial class of lignin-degrading enzymes and are copper-containing enzymes capable of oxidizing electron-rich organic substrates such as lignin using molecular oxygen as an electron acceptor. The genome of *Cerrena unicolor* was recently added to the JGI MycoCosm database and has eight laccases. Two of these laccases, designated Lc1 and Lc2, predicted to have the highest likelihood for successful expression in soluble, active form were selected for characterization. Lc1 and Lc2, which share 65% sequence identity, were heterologously expressed in *Komagataella pastoris*

(formerly *Pichia pastoris*), allowing characterization and comparison of their purified forms. Lc1 and Lc2 had half-lives of 16 min and 185 min at 60°C, respectively, and, based on molecular dynamics simulations, the longer half-life of Lc2 was due to an increased number and persistence of salt bridges compared to Lc1. Using model lignin-like dimers and a nanostructure-initiator mass spectrometry assay to quantify catalysis of specific bond-breaking events, both Lc1 and Lc2 had their highest activity at pH 3 and in combination with syringaldehyde as a mediator, with Lc1 having a higher catalytic efficiency of β-O-4' ether and C-C bond breaking. This comparative study demonstrates the diversity, including thermostability differences, of laccases from the same fungus, and improves our understanding of laccase catalyzed breaking of bonds commonly found in lignin, which will facilitate the developing this important class of enzymes for applications in the conversion of lignin to valuable bioproducts.

Keywords
Laccase; lignin; nanostructure-initiator mass spectrometry (NIMS); fungi; *Komagataella pastoris* (formerly *Pichia pastoris*); *Cerrena unicolor*

1. Introduction

Lignin is the most abundant renewable source of aromatics on earth [1], and converting it to valuable products is paramount to building an economically viable renewable biofuels industry [2]. As a first step in the process of converting lignin to valuable products, it must first be depolymerized to biologically available intermediates [3, 4]. In nature, fungi and bacteria produce an array of enzymes, including laccases, lignin peroxidases (LiP), versatile peroxidases (VP), and manganese peroxidases (MnP), that are secreted into the environment and catalyze reactions required to break both ether and carbon–carbon bonds in phenolic (10-30% in lignin polymer) and non-phenolic lignin subunits (79-90% in lignin polymer) [5-7]. Thus, potential biological routes to lignin conversion begin with depolymerization of lignin using natural lignin-degrading enzymes derived from secretomes of white-rot fungi [8, 9], but complex interactions among the different agents in secretomes can lead to difficulties in elucidating the mechanisms of lignin-degrading enzymes and make it particularly difficult to compare enzymes from either the same enzyme family or from the same fungus. Therefore, instead of mixed secretomes of ligninolytic enzymes, heterologous expression of individual genes, purification of the resulting enzymes, and quantification of bond-breaking events is a valuable approach to studying and comparing the structure-function relationships of these essential enzymes and to building potent enzyme mixtures for efficient lignin depolymerization. In this study, laccases from the white rot causing basidiomycete *Cerrena unicolor* were heterologously expressed in *Komagataella pastoris* (formerly *Pichia pastoris*) and characterized on a variety of substrates.

Laccases (EC 1.10.3.2) are copper-containing enzymes capable of oxidizing various electron-rich organic and inorganic substrates using molecular oxygen as an electron acceptor and are found in plants, fungi, and bacteria [10]. In plants, laccases participate in the radical-based mechanisms of lignin polymer formation [11, 12], while in fungi, they play critical roles in several physical functions

such as morphogenesis, fungal plant-pathogen/host interaction, stress defense, and lignin degradation [13]. In comparison, bacterial laccases are involved in pigmentation processes, morphogenesis, toxin oxidation, and protection against oxidizing agents and UV light [14, 15], and they have been used in bioremediation, mainly for the degradation of synthetic dyes [16-18].

Fungal laccases, principally those from white-rot fungi, are of particular interest for lignin depolymerization due to having higher redox potential compared with bacterial laccases [19, 20]. Among fungi, white-rot basidiomycetes are the most efficient lignin degraders and laccase producers [21, 22], and well-studied laccase-producing basidiomycetes include *Pleurotus ostreatus* [23], *Trametes versicolor* [24], *Agaricus bisporus* [25], *Coprinopsis cinerea* [26], *Ganoderma lucidum* [27]. Laccases have also been identified in soil ascomycetes from genera including *Aspergillus, Curvularia*, and *Penicillium* [28-30] and in bacterial genera such as *Bacillus, Streptomyces, Klebsiella, Pseudomonas, Yersinia, Proteobacterium,* and *Marinomonas* [14, 17].

Cerrena unicolor is a globally distributed and aggressive wood-decaying white-rot fungus found on hardwoods. It has evolved to decompose woody plant material under various environmental conditions by adjusting its metabolism to grow on different types of wood [31]. Several studies have reported on *C. unicolor* production of laccases and their application in dye decolorization and denim bleaching [32-34]. However, only a few reports have studied the degradation of lignin by *C. unicolor* laccases, and there is no experimental evidence that the recombinant and purified laccases from *C. unicolor* catalyze the breaking of bonds commonly found in lignin. Recently, a study by Longe et al. (2018) reported that incubation of unpurified laccase from the secretomes of *C. unicolor* with organosolv lignin resulted in 49% and 73% decreases in the average molecular weight (Mn) with 2,2’-azinobis(3-ethylbenzthiazoline-6-sulfonic acid (ABTS) and violuric acid as mediators, respectively. However, 14-15% of oxidized S-unit β-O-4' bond content was observed after enzyme treatment in the presence of violuric acid as a mediator rather than β-O-4' bond-cleavage. Furthermore, phenolic products were not detected, so elucidating the degradation mechanism was not possible in this study [34].

This work aimed to improve our understanding of the mechanism underlying laccase catalyzed depolymerization of lignin by comparing and contrasting two sequence diverse laccases from *C. unicolor*. The structure-based selection of the two novel laccases, designated as Lc1 and Lc2, from a *C. unicolor*, their expression in Komagataella pastoris, and a comparison of their catalytic performance, thermal stability, and solvent stability are presented. Data on the effect of a natural mediator, syringaldehyde, on bond cleavage frequency are also reported. Monitoring and quantification of catalysis of breaking β-O-4' ether bonds, C_α-C_β bonds, and C_α-C_1 carbon bonds (ring A) and production of by-products from C_α-oxidation and polymerization of reaction products was achieved using a recently developed nanostructure initiator mass spectrometry (NIMS) assay for quantifying the breaking of ether and C-C bonds in lignin-like model compounds [35, 36]. The utility of this assay was recently demonstrated in a study showing how pH can be used to control peroxidase catalysis of β-O-4' ether and C-C bonds in lignin model compounds [37].

This report provides a fundamental knowledge and comparison of two sequence diverse laccases from *C. unicolor*, which improves our understanding of the diversity of laccases from *C. unicolor* and in general, our understanding of laccase catalyzed breaking of specific bonds found in lignin. Improved understanding of laccase catalyzed lignin depolymerization reactions also facilitates developing this important class of enzymes for applications in converting lignin to valuable products and use in biorefinery implementations.

2. Materials and Methods

2.1 Selection of Laccase Genes from Genome Data

Eight laccase genes from the genome of *C. unicolor* were identified in the JGI – MycoCosm database (https://mycocosm.jgi.doe.gov/Cerun2/Cerun2.info.html) [38]. Structures for the proteins were homology modeled using the SWISS-MODEL web server [39] with PDB ID 5z1x, which has greater than 60% sequence identity to all target sequences, as a template. The protonation states of titratable residues were predicted using PROPKA at pH 6.0 [40, 41]. Protein solubilities were predicted using Aggrescan3D (A3D) 2.0 webserver (http://biocomp.chem.uw.edu.pl/A3D2/) [42] with parameters set to include stability calculations, non-dynamic modes, and a distance of aggregation of 5 Å.

2.2 Cloning of Laccase Isozymes

Genes were codon-optimized and synthesized by Genscript Co. (USA). Genes with recognition sites for XhoI and EcoRI restriction sites were cloned into the pPICZαA vector from Invitrogene™ (Life Technologies, USA). The N-termini of each protein was constructed to contain the Kex2 signal cleavage site at the end of the α-factor secretion signal from *Saccharomyces cerevisiae*. The cloned vectors pPICZαA-Lc1 and pPICZαA-Lc2 were linearized with *PmeI* and *SacI*, respectively, and transformed into *K. pastoris* KM71H strain by chemical transformation as described in the Pichia Expression Kit User Manual (Life Technologies, USA).

Transformed colonies were grown at 30°C on yeast extract peptone dextrose medium with sorbitol (YPDS) agar plates containing 100 µg/ml Zeocin™ antibiotic. Positive colonies were streaked out on YPDS agar plates containing higher concentrations of Zeocin™ and clones on plates with 1000 µg/ml Zeocin™ were chosen for further experiments.

2.3 Expression of Laccase Isozymes

K. pastoris KM71H transformants were grown in buffered complex methanol medium (BMMY) overnight at 30°C at 200 rpm. The overnight inoculation was used for the main culture of 50 ml BMMY in 250-ml flasks, and *K. pastoris* was grown to an OD_{600} of 0.6. The cultures were shaken at 30°C and 200 rpm for 3-5 days. The medium was fed daily with a 1% (v/v) methanol solution and 1 mM $CusO_4$ in the final concentration. Cell cultures were stopped when the laccase activity, measured as oxidation of ABTS substrate, reached saturation levels.

2.4 Purification of Recombinant Lc1 and Lc2 Enzymes

Culture supernatants were collected by centrifugation (9000 rpm for 15 mins) and clarified with 0.2 µm membrane filtration. The clarified supernatant was 15X-concentrated using Amicon® Ultra-50-kDa Centrifugal Filter Units. The concentrated enzyme solution was dialyzed through a 10-kDa membrane overnight against 100 mM sodium acetate (pH 3.0) at 4°C to partially remove impurity proteins, then again dialyzed overnight against 10 mM sodium acetate (pH 6.0) at 4°C. The precipitate was removed by centrifugation at 13,000 rpm for 15 mins and filtered through 0.2 µm membrane filtration before being loaded onto the Hitrap-Q XL (5 ml) column with an AKTA FPLC (GE Healthcare, UK) purification column. Stepwise gradients of buffer A (10 mM sodium acetate, pH 6.0)

and buffer B (500 mM sodium acetate, pH 6.0) were set up to pool active fractions. The most active fractions towards ABTS oxidation were collected for further characterization.

2.5 Biochemical Characterization

Protein concentrations were estimated using Pierce™ BCA Protein Assay Kits (Thermo Scientific, USA). A 12% denatured-PAGE of the most active fractions from the purification step was run and stained with SimplyBlueTM SafeStain reagent (Life Technologies, USA). The native-PAGE gel was also used for zymograms, where oxidation of ABTS was measured by incubating the gel slab in 100 mM sodium acetate buffer (pH 3.0) containing 1 mg/ml ABTS, to ensure the protein bands at the expected molecular weights were the active laccases. Protein deglycosylation reactions were performed using Protein Deglycosylation Mix II (New England Biolabs, USA) in non-denaturing conditions at 30°C for 24 hours to remove all N-linked O-linked glycans.

Laccase activity was assayed in 100 mM volumes at pH 3-6 in sodium acetate buffer, at pH 7-8 in sodium phosphate buffer, and pH 9-10 in sodium carbonate buffer. Thermostability was measured by incubating the protein at 60°C and pH 6.0 (100 mM sodium acetate) for 24 hours and measuring residual laccase activity after incubation using the ABTS oxidation assay and comparing activity to initial activity at t = 0. The residual enzyme activity was determined at room temperature in 100 mM sodium acetate buffer (pH 3.0) with 1 mg/ml ABTS. The increased absorbance from the formation of cationic radical $ABTS^{+\cdot}$ was recorded at 420 nm (ε = 36 mM^{-1} cm^{-1}) [43]. One unit (U) of activity was defined as the production of 1 µmol of product per minute under the reaction condition of 25°C and pH 3.0. Enzyme activity was calculated using the following equation, where the blank sample was the buffer used for enzyme preparation:

$$\mathrm{OD}_{420\mathrm{nm}} = \mathrm{Abs}_{\text{enzyme+substrate solution}} - \mathrm{Abs}_{\text{blank sample+substrate solution}} - \mathrm{Abs}_{\text{subtrate solution}}$$

$$\text{Activity}\left(\frac{\text{Unit}}{\text{ml}}\right) = \frac{OD\ x\ [reaction\ volume, ml)}{36\ x\ [incubation\ time, , min]\ x\ \{laccase\ volume, ml)}$$

Kinetic parameters for LC1 and LC2 were determined for oxidation of ABTS and for oxidation of 2,6-dimethoxyphenol (DMP), two compounds commonly used for measuring the kinetics of laccases. Assays were conducted at substrate concentrations ranging from 50 to 2000 µM, and the reaction was initiated by adding 0.02 µM enzyme at 25°C. ABTS and DMP oxidation was determined by measuring absorbance at 420 nm (ε = 36,000 M^{-1} cm^{-1}) and 468 nm (ε = 49,600 M^{-1} cm^{-1}), respectively [43]. Net oxidation rates were measured as the difference between the amount of substrate consumed in the presence of enzyme and the amount consumed in the absence of enzyme. Data are reported as the mean and standard error of triplicate experiments. Steady-state kinetic parameters were obtained from the rearrangement of the Hanes–Woolf plot from the Michaelis–Menten equation.

2.6 Enzyme Reactions with the Fluorous-Tagged Phenolic B-O-4 Linked Model Compound

The phenolic β-O-4 aryl ether lignin-like model compound, NIMS-tagged guaiacylglycerol-beta-guaiacyl ether (GGE, Figure 1), was synthesized according to a previously established protocol [35]. Enzyme reactions with the NIMS-tagged GGE (1 mM) were performed at pH 3.0-10.0 in the pH appropriate buffer (see section 2.5) and in the absence and presence of 20 mM of syringaldehyde

as a mediator. The reaction was quenched after 3 hours, and reaction products were analyzed using nanostructure-initiator mass spectrometry (NIMS) as previously described [35].

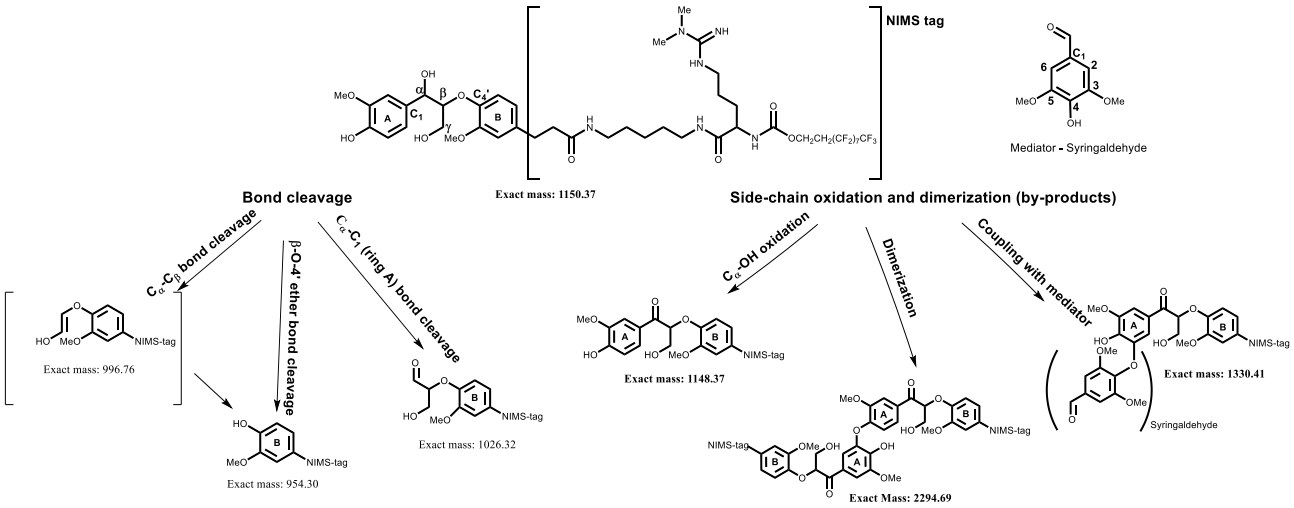

Figure 1 Structures and molecular weights for the NIMS tagged model phenolic lignin dimer (top half) and products from laccase (Lc1 or Lc2) catalyzed bond breaking and polymerization due to the coupling reaction between the lignin dimer and mediator in the presence of mediator syringaldehyde (bottom half).

2.7 Molecular Dynamics Simulations

Molecular dynamic (MD) simulations were performed using NAMD ver. 2.1 [44] and the CHARMM36 forcefield [45]. The protonation states of the modeled structures of Lc1 and Lc2 titratable residues were predicted using PROPKA at pH 6.0 [40, 41]. The models were solvated in a box of TIP3P water molecules that extended 10 Å from the surface of the protein structure (8023 and 9261 water molecules for Lc1 and Lc2, respectively). Counterions (Na^+, Cl^-) were added to achieve a NaCl concentration of 0.1 M. MD simulations were run with periodic boundary conditions at a constant temperature of 333.15°K and atmospheric pressure using a Langevin thermostat [46]. The Particle Mesh Ewald method was applied to account for long-range electrostatic interactions at a cutoff distance of 12 Å [47]. Solvated proteins were energy minimized for 10 ps and then gradually heated to the desired temperature (333.15°K) over 300 ps. The system was then equilibrated at 333.15°K for 5 ns under an isothermal−isobaric ensemble (NPT), followed by a 50 ns production run in the canonical (NVT) ensemble. Snapshots were collected at 5 ps intervals during the last 20 ns of the MD simulation. Root-mean-square deviation (RMSD), per-residue root-mean-square fluctuation (RMSF) and salt-bridge networks were analyzed using VMD software [48].

3. Results and Discussions

Cerrena unicolor, commonly known as the mossy maze polypore, is a saprobic fungus that causes white rot on the deadwood of hardwoods. The genome of *Cerrena unicolor* was recently deposited into the JGI – MycoCosm database (https://mycocosm.jgi.doe.gov/Cerun2/Cerun2.info.html) and contains eight genes annotated as laccases [38]. Two of these laccases were chosen for detailed characterization based on predictions of their aggregation propensity and were characterized for their thermostability and activity as a function of pH and the presence of the mediator

syringaldehyde. Differences in stability and activity were studied using molecular dynamics simulations.

3.1 Identification of Low Aggregation Propensity Laccases

Heterologous expression of fungal laccases has proven difficult and, along with a lack of assays that allow quantification of specific bond-breaking events, has been a significant bottleneck to studies of their structure and function. During overexpression of genes in a host cell, high protein abundance, close physical interaction, and specific properties of the protein such as high hydrophobicity, the high propensity of β-sheets, low net charge, and intrinsically disordered regions of protein structure can result in an increased likelihood of aggregation [49-51]. Working under the hypothesis that aggregation is a significant reason for the low heterologous expression of fungal laccases, structures of all eight laccases were homology modeled and their aggregation propensities were calculated using the Aggrescan3D web server [51]. Two laccases designated Lc1 (protein ID 383410) and Lc2 (protein ID 408157), had the lowest aggregation propensity scores (Table 1) and were selected for characterization. Lc1 and Lc2 contain 516 and 525 amino acids, respectively, have ~65% sequence identity and each is predicted to have a putative signal peptide of 21 amino acids, which was predicted using SignalP-5.0 Server [52]. In addition, these laccases each contain 2-3 potential N-glycosylation sites, which were predicted using the NGlycPred Server [53] (Supplementary data, Figure S1).

Table 1 Annotated laccases from the genome of *C. unicolor* V1.1 (JGI – MycoCosm data source, https://mycocosm.jgi.doe.gov/Cerun2/Cerun2.info.html) and their predicted aggregation propensity scores. Homology models were created using the SWISS-MODEL web server with template PDB ID 5Z1X. Aggregation propensity scores were predicted using Aggrescan3D (A3D) 2.0.

Protein ID	Transcript ID	Location	Total score value
193382	193597	Scaffold_52:14136-16554 (-)	-76.3717
310741	310956	Scaffold_9:221275-223444 (+)	-91.7623
357631	357846	Scaffold_25:271860-274236 (-)	-86.8936
364416	364631	Scaffold_87:11000-13198 (-)	-95.4062
383410 *(Lc1)*	383625	Scaffold_52:10660-13119 (-)	-120.8213
390832	391047	Scaffold_87:25066-27238 (+)	-79.2469
408157 *(Lc2)*	408372	Scaffold_9:514822-516993 (-)	-131.7249
448635	448850	Scaffold_49:113863-116800 (+)	-89.0249

3.2 Recombinant Expression and Purification of Lc1 and Lc2

Expression was carried out in volumes of 150 ml in 500-ml flasks and oxidation of ABTS in the extracellular supernatant over the three to four-day culture was used to quickly ascertain whether soluble, active laccase was being secreted. Laccase activity measurements reached their maximum

values of 599.5 U/L and 382.1 U/L after 3 days for Lc1 and Lc2, respectively (Figure 2). The negative control with *K. pastoris* transformant containing only the blank pPICZαA vector had no activity toward oxidation of ABTS (data not shown).

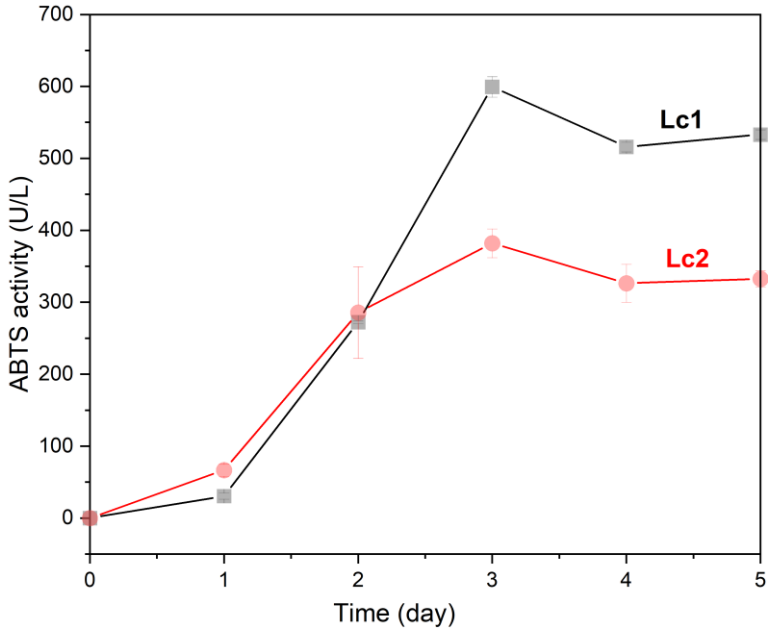

Figure 2 Time course of oxidation of ABTS catalyzed by laccases secreted into the supernatant of *K. pastoris* strain containing *Lc1* gene (black curve) and *Lc2* gene (red curve). Assay conditions: ABTS in concentration of 1 mg/ml in sodium buffer 0.1 M, pH 3.0, and at 25°C. The increased absorbance from the formation of cationic radical $ABTS^{+\cdot}$ was recorded in 2 mins at 420 nm (ε = 36 mM^{-1} cm^{-1}). Data are the means and standard deviations for triplicate experiments.

Recombinant Lc1 and Lc2 were purified using anionic exchange chromatography. The total unit of activity toward ABTS was not changed after the dialysis step (data not shown). After anionic exchange chromatography, native PAGE analysis revealed that the molecular masses of purified Lc1 and Lc2 were approximately 110 kDa, which were much higher than the calculated molecular weights of 55.9 kDa and 57.6 kDa for Lc1 and Lc2, respectively (Figure 3). This suggested Lc1 and Lc2 were potentially glycosylated at one or more of the 2-3 predicted glycosylation sites when expressed in *K. pastoris.* The higher-than-expected molecular weights could also occur if LC1 and LC2 formed dimers in the denatured gel. Furthermore, laccase zymograms with ABTS revealed strong bands in the same molecular weight positions, indicating these bands corresponded to active laccases, and the Lc1 zymogram showed higher activity than Lc2 toward ABTS at pH 3.0.

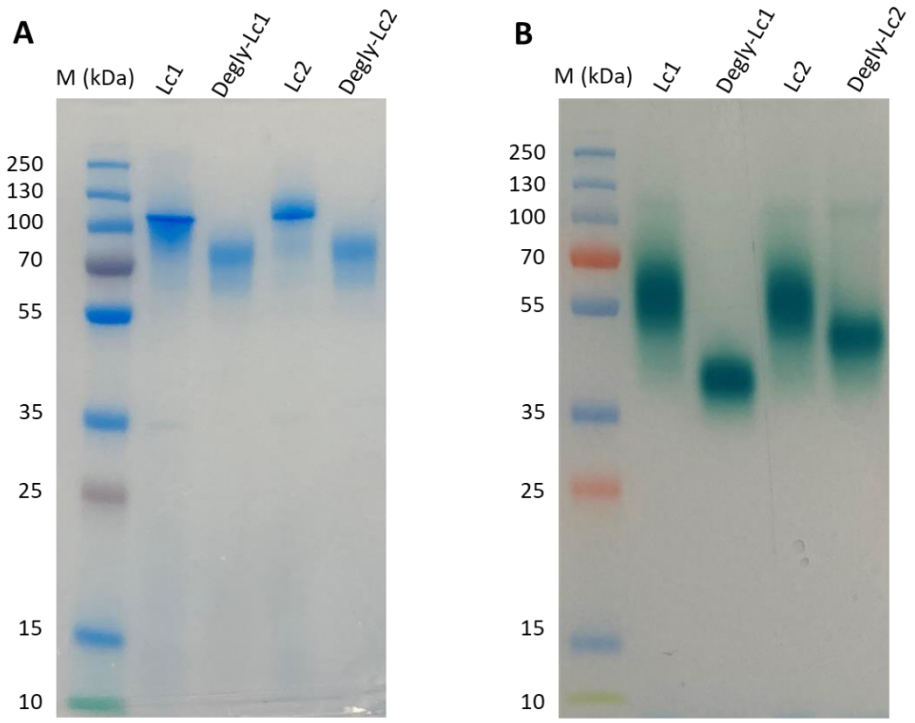

Figure 3 PAGE gels of the purified intact Lc1, Lc2, and their deglycosylated forms. Lane M contains protein molecular weight markers. (A) Coomassie-stained denatured PAGE gel of intact Lc1, Lc2, and deglycosylated Lc1, and Lc2, indicating Lc1 and Lc2 are glycosylated. (B) Zymogram (native-PAGE) of intact Lc1, Lc2, and their deglycosylated forms stained with ABTS (1 mg/ml) in 100 mM sodium acetate buffer pH 3.0, showing both forms catalyze the oxidation of ABTS.

3.3 Biochemical Characterization

3.3.1 pH Stability

The stability of Lc1 and Lc2 as a function of pH was studied by incubating the enzymes for 24 hours at pH ranging from 3-10 and measuring residual activity using the ABTS oxidation assay. Generally, Lc1 showed the highest stability and activity over pH 6-8 and was less stable at pH 3-5 and pH 9-10. The stability of Lc2 was higher at neutral and basic pH values (pH 7-10) than at acidic pH values (3-6). After 24 hours incubation at pH 3 Lc1 and Lc2 retained 44.8% and 59.3% of their initial activity (incubation time = 0 hours), respectively. After incubation for 24 hours at pH 10, Lc1 retained 21.6% of its activity, while Lc2 retained 95.5% of its activity (Figure 4A). Bacterial laccases are typically stable at pH ranging from neutral to alkaline (pH 6-11) [54] while fungal laccases are typically more stable under acidic pH [55, 56]. The two *C. unicolor* laccases studied here showed stability over a broad pH range of 6-10, suggesting they could be good options for use on various substrates coming from biomass conversion and contaminated waste streams such as textile effluents [56] that will potentially have very different pH due to the pretreatment process employed.

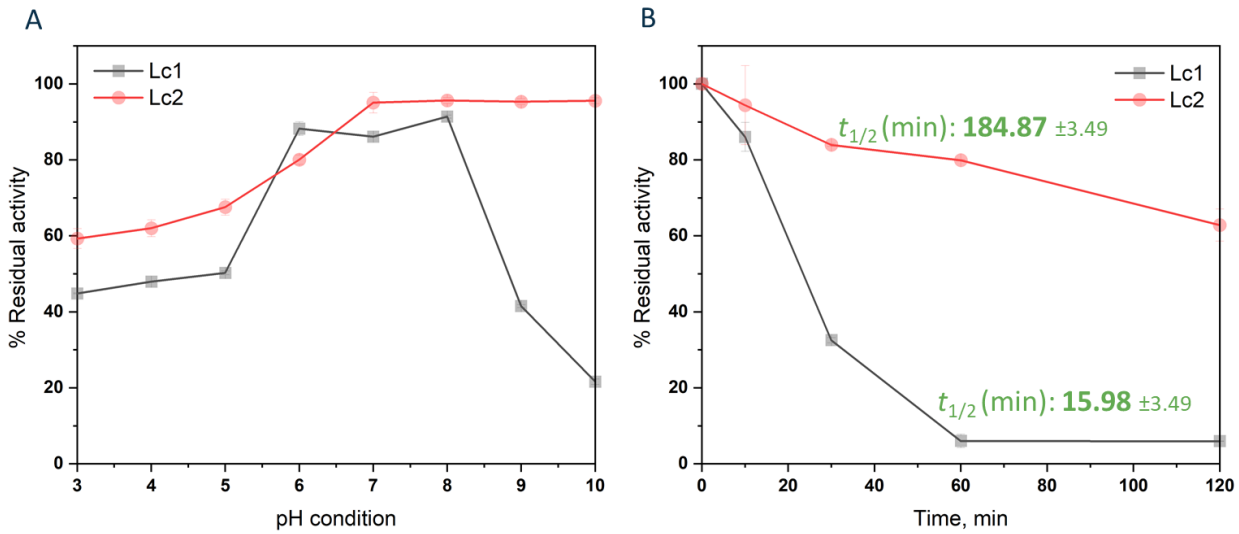

Figure 4 pH and thermal stability of Lc1 and Lc2. (A) pH stability was measured as residual activity toward oxidation of ABTS after incubation of the enzyme at the indicated pH for 24 hours and (B) thermal stability of Lc1 and Lc2 was measured as residual activity toward oxidation of ABTS after incubation of the enzyme at the indicated temperature for 2 hours. The data presented are the mean and standard derivation from triplicate experiments.

3.3.2 Thermostability

The thermostabilities of Lc1 and Lc2 were examined by measuring residual enzyme activity on oxidation of ABTS after incubation for 2 hours at 60°C and pH 6.0 and determining the half-life of each enzyme. Lc2 was very stable at 60°C with a half-life of 184.87 min, while Lc1 lost half of its activity after only 15.98 min at 60°C (Figure 4B). A few thermostable laccase isoenzymes have previously been isolated, including laccase isoenzymes from *Fomes sclerodermeus, T. hirsutus, Coliolus zonatu, Marasmius quercophilus, Myceliophtora thermophile, and Scytalidium thermophilum* [44, 45]. Other laccases from *Trametes trogii* BAFC 463, *C. unicolor* BBP6 have been observed and expressed in *P. pastoris* [32, 46]. The laccase from *C. unicolor* BBP6 retained approximately 30% of its activity on ABTS after 2 hours of incubation at 60°C [32], whereas Lcc3 from Trametes trogii BAFC 463 exhibited a half-life of 3 hours at 60°C [46], which are both comparable to Lc2 from *C. unicolor* reported in this study.

3.3.3 Molecular Dynamics (MD) Analysis of Stability

MD simulations of Lc1 and Lc2 were conducted at 333.15°K (60°C) to gain insights into the relationships between protein structure and thermostability. Metrics including overall protein flexibility and the number and persistence time of salt bridges were used to explain differences in their thermostabilities. Higher root mean square deviation (RMSD) and per-residue root mean square fluctuation (RMSF) were observed for Lc1 than for Lc2 (Supplementary data, Figure S2), which supported the experimental data that showed Lc2 was more thermostable than Lc1. In the Lc1 structural model, increased flexibility was observed for adjacent residues (aa 300-400) located on the protein surface, where this region is more likely to be easily disrupted by heat and solvent

interactions (Supplementary data, Figure S2B). Salt bridge interactions also play an essential role in stabilizing protein structures where they stabilize structural and functional conformations and are altered by changes in pH [57, 58]. Ionic bonds (salt bridges) were detected when a positively charged nitrogen atom of lysine (NZ) or arginine (NH1, NH2) or positively charged histidine (HIP: ND1 NE2, both protonated) was within 3.2 Å of a negatively charged oxygen atom of glutamate (OE1, OE2) or aspartate (OD1, OD2). The structural models of Lc1 and Lc2 had 35 and 43 salt bridges, respectively, with 24 salt bridges in homologous positions (Supplementary data, Table S1). The persistence time of the homologous salt bridges in Lc1 and Lc 2 were also compared over the MD production run. These results showed that at 333.15°K, in Lc2, a more significant number of salt bridges persisted for a longer time than in Lc1 (Figure 5), which provides additional insights into Lc2 being more stable than Lc1 at higher temperatures.

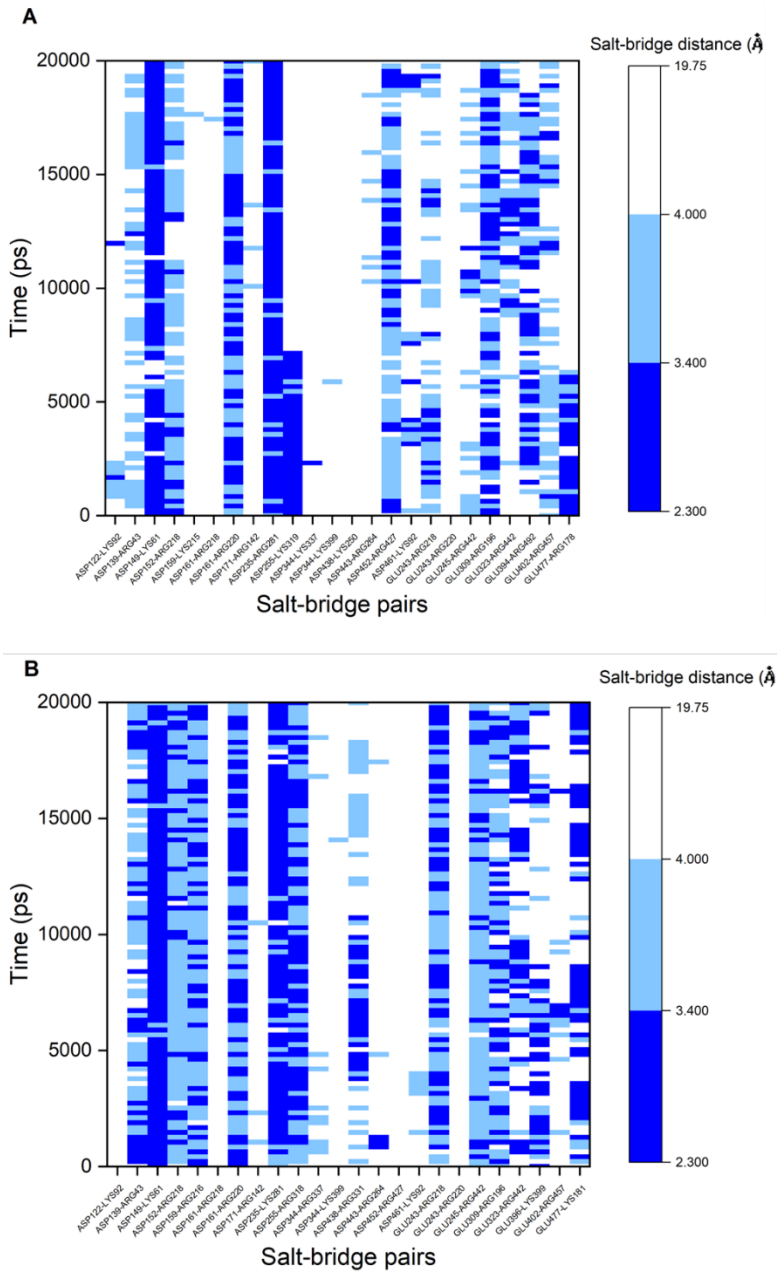

Figure 5 Time dependence of the network of salt bridges over the last 20 ns of the molecular dynamics production runs for Lc1 and Lc2.

3.3.4 Oxidation of Aromatic Compounds

The kinetic parameters for laccases Lc1 and Lc2 with 2,6-DMP and ABTS are presented in Table 2. Generally, both Lc1 and Lc2 had higher affinity (K_m) and catalytic efficiency (k_{cat}/K_m) on ABTS oxidation compared to catalysis of DMP oxidation. Catalytic efficiency with ABTS as substrate was 6.3 times and 13.2 times higher than with DMP as a substrate for Lc1 and Lc2, respectively. In more detail, Lc1 and Lc2 exhibited similar K_m values toward ABTS and DMP; however, their k_{cat} values were different. The k_{cat} values of Lc1 are 2.0 times and 5.4 times higher than those for Lc2 with ABTS and DMP as substrates, respectively. The kinetics parameters of Lc1 and Lc2 were compared with those of other fungal laccases assayed under similar reaction conditions and in which laccases, in general, have high oxidation efficiency of ABTS and DMP. A wide range of K_m and k_{cat} for ABTS and DMP have been reported for fungal laccases [59], and all the parameters reported for Lc1 and Lc2 in this study were in the range for those for laccases from other white-rot fungi. For reference, the k_{cat} spans several orders of magnitude for different fungal laccases, with the laccase POXA3b from *P. ostreatus* having the highest k_{cat} (1.58E+05 s^{-1}) [60] and the laccase from *T. hirsuta* having the lowest k_{cat} (196 s^{-1}) toward oxidation of ABTS at pH 5.0, 25°C [61].

Table 2 Kinetic parameters for oxidation of ABTS and DMP by laccases Lc1 and Lc2 from *C. unicolor*. Data presented are the mean and standard deviation of triplicate experiments.

	ABTS			**DMP**		
	K_m (mM)	k_{cat} (s^{-1})	k_{cat}/K_m (s^{-1} mM^{-1})	K_m (mM)	k_{cat} (s^{-1})	k_{cat}/K_m (s^{-1} mM^{-1})
Lc1	0.158 ± 0.003	2036.1 ± 64.1	1.289E+04 ± 625.1	0.317 ± 0.024	642.8 ± 27.3	2.031E+03 ± 71.9
Lc2	0.229 ± 0.018	992.5 ± 13.5	4.350E+03 ± 417.9	0.363 ± 0.008	119.1 ± 3.91	3.281E+02 ± 8.1

3.3.5 Catalysis of Bond Breaking Using NIMS Assays

One of the rate-limiting steps in the degradation of lignin by laccases is the first electron transfer from lignin to the T1 copper of the laccase (T1Cu in Figure 6). The steric hindrance of bulky lignin substrates can result in low contact with T1 copper and its surrounding active sites [62]. In this case, small phenolic molecules, some of which have been reported to be products of oxidative degradation of lignin, can function as mediators and shuttle electrons between the enzyme and lignin macromolecule [63-65]. Among the three types of potential mediators, syringyl (S), guaiacyl (G), and *p*-hydroxyphenyl (H), S mediators are potentially the best choice because they are naturally occurring compounds that have lower redox potential and yield lower repolymerization of lignin fragments due to the occupation of the C5 position by a methoxy group [66]. In previous studies, using syringaldehyde as a mediator maximized release of S-unit derivatives during both biological degradation (57) and chemical oxidative depolymerization of S-rich lignin such as hardwoods (58-60). Previously published papers also showed that natural mediators such as syringaldehyde improved laccase-catalyzed breakdown of phenolic lignin model compounds and decolorization of different types of recalcitrant dyes [67-69]. Thus, in the work presented here, the effects of

syringaldehyde on the distribution of specific laccase-catalyzed bond breaking in model lignin dimers were studied.

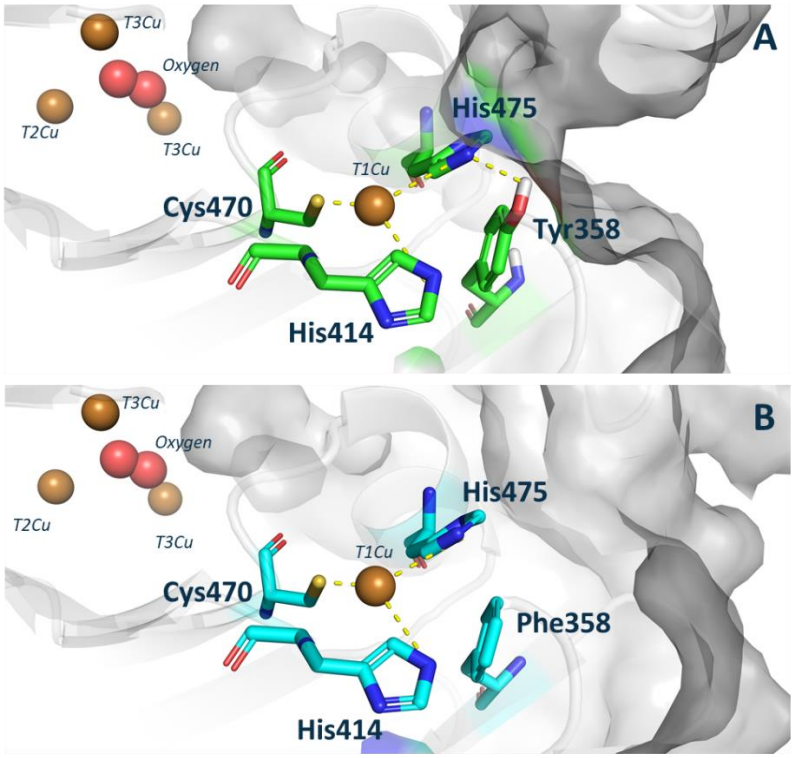

Figure 6 Active sites of Lc1 (A) and Lc2 (B). Cu sites are colored as reddish-brown spheres, and oxygen molecules are colored as a red sphere. Residues in the vicinity of the T1Cu site are depicted as sticks.

Previous publications on laccase isozymes from the lignin-degrading fungus *C. unicolor* [70, 71] presented studies on only catalysis of ABTS oxidation. This study, in addition to reporting on Lc1 and Lc2, catalyzed oxidation of ABTS and DMP, reports on their ability to catalyze the breaking of bonds commonly found in lignin using model dimers as substrate and quantifying bond breaking using our recently developed nanostructure-initiator mass spectrometry assay [35, 36]. Results on the increased activity of Lc1 and Lc2 when syringaldehyde was used as an electron transfer mediator in the degradation of the lignin-like model dimer are also presented. Breaking of β-O-4' ether, C_α-C_1, and of C_α-C_β bonds were quantified by analyzing products with masses m/z 954.30, m/z 1026.32, and m/z 996.76, respectively. Other by-products (side-chain oxidation and dimerization) were also detected (Figure 1). As a result (Figure 7A and Figure 8A), both Lc1 and Lc2 directly interacted with the phenolic model lignin-like dimer and produced products from breaking of both β-O-4' ether and C_α-C_1 bonds in the absence of a mediator. At all pH levels, β-O-4' ether bond cleavage released a phenolic product (m/z 954.3, Figure 1), which was the dominant catalytic event, followed by C_α-C_1 carbon bond cleavage, C_α-OH oxidation, and a small amount of repolymerized product with the mediator. Both laccases showed very low activity toward the model dimer at alkaline pH (8-10), even in the presence of syringaldehyde (Figure 7B, Figure 8B). At pH 10, 90.5% and 80.6% substrate and polymers remained at the end of the reaction for Lc1 and Lc2, respectively.

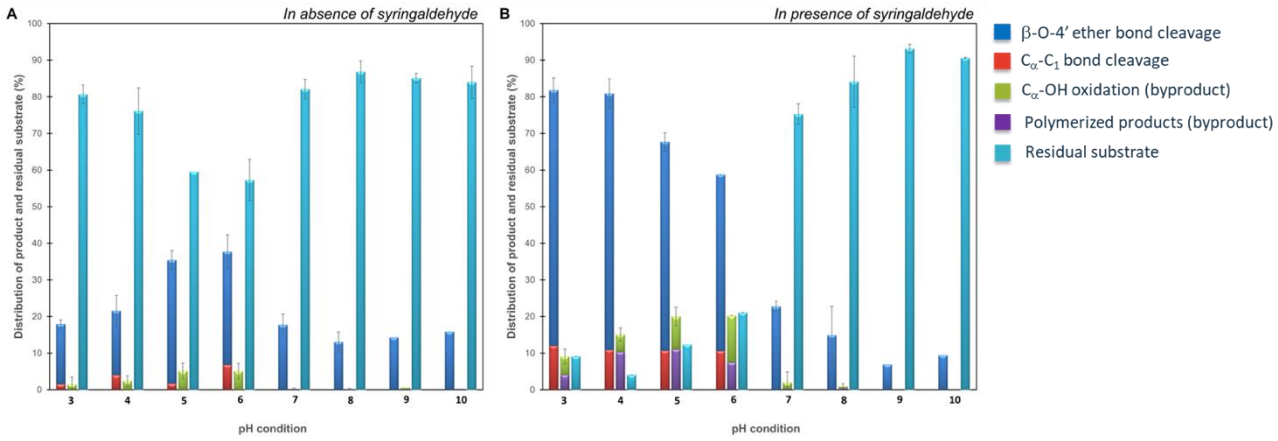

Figure 7 Product distribution from Lc1-catalyzed degradation of the model lignin dimer (Figure 1) in the absence (A) and presence (B) of syringaldehyde at different pH. The data presented are the mean and standard deviation for three replicates. To better compare the dominant reactions to side reactions, the first column at each pH is the mean and standard deviation of the products from both β-O-4' ether and C_α-C_1 bond breaking, and the second column at each pH is the mean and standard deviation of the products from both C_α-OH oxidation and polymerized product combined.

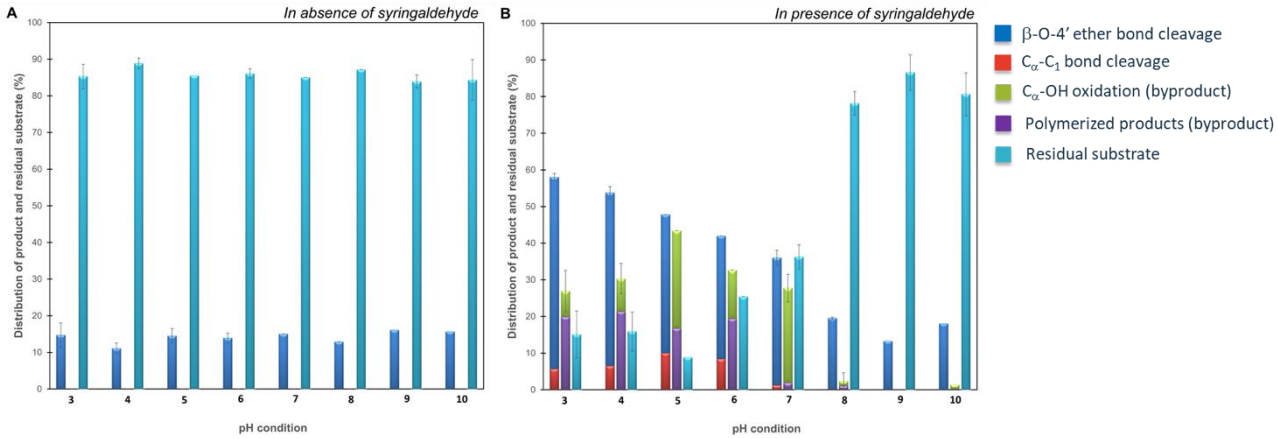

Figure 8 Product distribution from Lc2-catalyzed degradation of the model lignin dimer (Figure 1) in the absence (A) and the presence (B) of syringaldehyde at different pH. The data presented are the mean and standard deviation for three replicates. To better compare the dominant reactions to side reactions, the first column at each pH is the mean and standard deviation of the products from both β-O-4' ether and C_α-C_1 bond breaking, and the second column at each pH is the mean and standard deviation of the products from both C_α-OH oxidation and polymerized product combined.

Figure 7A and Figure 7B show a comparison of Lc1 catalyzed breaking of bonds in the phenolic model compound in the absence (Figure 7A) and presence (Figure 7B) of the mediator syringaldehyde. In general, the presence of syringaldehyde had a significant effect on the frequency of the four reactions quantified, especially under acidic to near neutral conditions (pH 3-6). At pH 3-6, the presence of syringaldehyde has a large impact on catalysis of both β-O-4' ether (Figure 7A and B, blue bars) and C_α-C_1 (Figure 7A and B, red bars) bond breaking, reaching a maximum combined

value of 82% conversion at pH 3-4 (Figure 7B, stacked red and blue bars) compared to only a maximum conversion of 35% at pH 5-6 (Figure 7A, stacked red and blue bars) in absence of syringaldehyde. C_α-OH oxidation (Figure 7, green bars) was only marginally increased at pH 5-6 by the presence of syringaldehyde. In presence of the mediator compounds associated with polymerization of breakdown products and possibly the mediator appeared (Figure 7B, purple bars). C_α-OH oxidation plus a product resulting from the polymerization of products produced from bond breaking accounted for 9% of detected masses. In contrast, Lc2 catalyzed breaking of only β-O-4' ether bonds at pH 3-10 without syringaldehyde, converting only 15% of the phenolic substrate (Figure 8A). In the presence of syringaldehyde, Lc2 catalyzed breaking of both β-O-4' ether and C_α-C_1 bonds, accounting for a maximum of 58.0% of products (Figure 8B, stacked red and blue bars at pH 3). Both C_α-OH oxidation and polymerized products appeared at pH 3-7 and constituted approximately 27% of the products (Figure 8B).

Since lignin contains both phenolic and non-phenolic compounds, catalysis of β-O-4' ether, C_α-C_1 and C_α-C_β bond breaking and of C_α-OH oxidation by Lc1 and Lc2 were also investigated using a NIMS-tagged non-phenolic compound. In these experiments, which were performed under the same conditions as the NIMS-tagged phenolic lignin dimer compound experiments, no products were observed regardless of whether syringaldehyde was included in the reaction.

Interestingly, in the absence of syringaldehyde, Lc1 exhibited a pH-dependent activity profile consistent with oxidation of the lignin-like model dimer (Figure 7A, Figure 8A). This result suggested that titratable residues at exposed active sites may play an essential role in the binding and oxidation of the lignin dimer. To investigate this, the homology models of Lc1 and Lc2 were superimposed. The T1Cu site of both laccases forms a three-coordinated trigonal planar model with His_{414}–Cys_{470}–His_{475}. In Lc1, there is an axial noncoordinating residue, Tyr_{358}, while in Lc2, this residue is replaced by Phe_{358} (Figure 6). It is well-known that the His–Cys–His tripeptide is responsible for electron transfer and axial noncoordinating residues such as Phe and Leu determine the redox potential of laccases [70]. These results suggested that a network of adjoining hydrogen bonds with only one of the aromatic amino acids with an ionizable side chain Tyr_{358} may play an essential role in determining the pH profile of laccase Lc1 through direct interaction with the phenolic lignin dimer. This active site complex could tune the energetically favorable cationic radical formation and stabilization by a proximal interaction between T1 active sites and mediator/lignin substrate in Lc1.

These results are consistent with studies showing that most fungal laccases have optimal activity toward phenolic compounds at pH 3-6, with sharp declines in activity at pH 6 and above [71-74]. Although a few engineered laccases with increased activity toward phenolic compounds such as 2,6-dimethoxyphenol and guaiacol at alkaline conditions (pH ≥ 8) have been reported, most of the reported laccases did not catalyze lignin depolymerization under alkaline conditions [75-77]. At alkaline pH, oxidation of phenolic compounds (either a phenolic mediator or a phenolic lignin dimer) to a phenoxy radical is favored by the presence of the phenolate form [64]. High pH also negatively affects laccase activity because the abundance of hydroxide anion has been shown to inhibit laccase due to competitive binding to T2/T3 coppers [78]. Furthermore, in neutral to alkaline conditions formation of phenoxy radical intermediates is favored over the formation of cationic radicals, resulting in a much higher bond dissociation energy and electron transfer rate with the mediator [37]. More understanding of the electron transfer mechanism and T2/T3-catalyzed molecular

oxygen reduction to water at the molecular level is needed for laccase engineering toward enhanced activity at alkaline pH.

4. Conclusions

In this study, the stability and catalytic properties of two laccases (Lc1 and Lc2) from the white rot causing basidiomycete *C. unicolor* were biochemically characterized and compared across a range of reaction conditions including pH, temperature, and presence of the natural mediator syringaldehyde. Interestingly, despite being from the same fungus and having ~65% sequence identity, the two laccases had very different thermostabilities and bond-breaking profiles, suggesting *C. unicolor*, and perhaps white rot fungi, in general, may have evolved laccase systems for optimal performance under varying environmental conditions. Specifically, Lc2 was stable and active over a broader pH range and had an ~10× longer half-life than Lc1. Molecular dynamics simulations showed these stability differences were largely due to differences in the number and persistence of hydrogen bonds and salt bridges and to Lc1 having a long and highly flexible surface loop from which unfolding may be initiated at lower temperatures. Breaking of ether and C-C bonds is critical to depolymerizing lignin into compounds amendable to uptake and conversion via engineered host organisms, and both Lc1 and Lc2 catalyzed breaking of β-O-4' ether, C_α-C_1, and of C_α-C_β bonds in a phenolic lignin-like model compound. Lc1 and Lc2 showed optimal activity under acidic conditions and were approximately four to five times more active when syringaldehyde was included in the reaction. Neither Lc1 nor Lc2 had the catalytic power to break these same bonds in the non-phenolic dimer, a result that was verified using the same non-phenolic dimer without the NIMS tag. This report provides a fundamental understanding and comparison of *C. unicolor* laccases, which improves our understanding of the diversity of laccases from *C. unicolor* and in general, our understanding of laccase catalyzed breaking of specific bonds found in lignin.

Acknowledgments

This work conducted at the Joint BioEnergy Institute was supported by the Office of Science, Office of Biological and Environmental Research, of the U.S. Department of Energy under Contract No. DE-AC02-05CH11231. This work was also supported by the Laboratory Directed Research and Development program at Sandia National Laboratories. Sandia National Laboratories is a multi-mission laboratory managed and operated by National Technology and Engineering Solutions of Sandia, LLC, a wholly-owned subsidiary of Honeywell International, Inc., for the U.S. Department of Energy's National Nuclear Security Administration under contract DE-NA0003525.

Author Contributions

LTMP and KLS conceived the study. LTMP designed and performed experiments and simulations. KD analyzed mass spectrometry. LTMP and KLS wrote the manuscript. TRN, SWS, BAS, and PDA discussed, revised, and edited the manuscript. All authors read and approved the final manuscript.

Funding

Office of Science, Office of Biological and Environmental Research, of the U.S. Department of Energy under Contract No. DE-AC02-05CH11231. Laboratory Directed Research and Development

program at Sandia National Laboratories. Sandia National Laboratories is a multi-mission laboratory managed and operated by National Technology and Engineering Solutions of Sandia, LLC, a wholly-owned subsidiary of Honeywell International, Inc., for the U.S. Department of Energy's National Nuclear Security Administration under contract DE-NA0003525.

Competing Interests

The authors have declared that no competing interests exist.

Additional Materials

The following additional materials are uploaded at the page of this paper.

1. Figure S1: Protein sequences of Lc1 and Lc2 from *Cerrena unicolor*. Amino acids in bold indicate a putative signal peptide. Predicted N-glycosylation sites are in blue.
2. Figure S2: Time course of RMSD for Lc1 and Lc2 (A) and per-residue RMSF flexibility (B) of Lc1 and Lc2 for 50 ns of MD simulation at 333.15 K. The inset image shows the surface loop for which the RMSF larger in Lc1.
3. Table S1: Salt-bridge network analysis for structural models of Lc1 and Lc2. The analysis was conducted using VMD software. Salt bridges were as defined as a negatively charged oxygen atom of an acidic residue being within 3.2 Å of a positively charged nitrogen atom of basic residue.

References

1. Xu Z, Lei P, Zhai R, Wen Z, Jin M. Recent advances in lignin valorization with bacterial cultures: Microorganisms, metabolic pathways, and bio-products. Biotechnol Biofuels. 2019; 12: 32.
2. Martinez-Hernandez E, Cui X, Scown CD, Amezcua-Allieri MA, Aburto J, Simmons BA. Techno-economic and greenhouse gas analyses of lignin valorization to eugenol and phenolic products in integrated ethanol biorefineries. Biofuels Bioprod Bioref. 2019; 13: 978-993.
3. Lin L, Wang X, Cao L, Xu M. Lignin catabolic pathways reveal unique characteristics of dye-decolorizing peroxidases in Pseudomonas putida. Environ Microbiol. 2019; 21: 1847-1863.
4. Kamimura N, Takahashi K, Mori K, Araki T, Fujita M, Higuchi Y, et al. Bacterial catabolism of lignin-derived aromatics: New findings in a recent decade: Update on bacterial lignin catabolism. Environ Microbiol Rep. 2017; 9: 679-705.
5. Janusz G, Pawlik A, Sulej J, Swiderska-Burek U, Jarosz-Wilkolazka A, Paszczynski A. Lignin degradation: Microorganisms, enzymes involved, genomes analysis and evolution. FEMS Microbiol Rev. 2017; 41: 941-962.
6. Lee S, Kang M, Bae JH, Sohn JH, Sung BH. Bacterial valorization of lignin: Strains, enzymes, conversion pathways, biosensors, and perspectives. Front Bioeng Biotechnol. 2019; 7: 209.
7. Hilgers R, Vincken JP, Gruppen H, Kabel MA. Laccase/mediator systems: Their reactivity toward phenolic lignin structures. ACS Sustain Chem Eng. 2018; 6: 2037-2046.
8. Salvachúa D, Martínez AT, Tien M, López-Lucendo MF, García F, de Los Ríos V, et al. Differential proteomic analysis of the secretome of irpex lacteus and other white-rot fungi during wheat straw pretreatment. Biotechnol Biofuels. 2013; 6: 115.

9. Martinez D, Challacombe J, Morgenstern I, Hibbett D, Schmoll M, Kubicek CP, et al. Genome, transcriptome, and secretome analysis of wood decay fungus Postia placenta supports unique mechanisms of lignocellulose conversion. Proc Natl Acad Sci U S A. 2009; 106: 1954-1959.
10. Solomon EI, Sundaram UM, Machonkin TE. Multicopper oxidases and oxygenases. Chem Rev. 1996; 96: 2563-2606.
11. Hoopes JT, Dean JFD. Ferroxidase activity in a laccase-like multicopper oxidase from liriodendron tulipifera. Plant Physiol Biochem. 2004; 42: 27-33.
12. Ranocha P, Chabannes M, Chamayou S, Danoun S, Jauneau A, Boudet AM, et al. Laccase down-regulation causes alterations in phenolic metabolism and cell wall structure in poplar. Plant Physiol. 2002; 129: 145-155.
13. Thurston CF. The structure and function of fungal laccases. Microbiology. 1994; 40: 19-26.
14. Liu Y, Huang L, Guo W, Jia L, Fu Y, Gui S, et al. Cloning, expression, and characterization of a thermostable and pH-stable laccase from Klebsiella pneumoniae and its application to dye decolorization. Process Biochem. 2017; 53: 125-134.
15. Mate DM, Alcalde M. Laccase: A multi-purpose biocatalyst at the forefront of biotechnology. Microb Biotechnol. 2017; 10: 1457-1467.
16. Blánquez A, Rodríguez J, Brissos V, Mendes S, Martins LO, Ball AS, et al. Decolorization and detoxification of textile dyes using a versatile Streptomyces laccase-natural mediator system. Saudi J Biol Sci. 2019; 26: 913-920.
17. Singh G, Bhalla A, Kaur P, Capalash N, Sharma P. Laccase from prokaryotes: A new source for an old enzyme. Rev Environ Sci Biotechnol. 2011; 10: 309-326.
18. Singh D, Rawat S, Waseem M, Gupta S, Lynn A, Nitin M, et al. Molecular modeling and simulation studies of recombinant laccase from Yersinia enterocolitica suggests significant role in the biotransformation of non-steroidal anti-inflammatory drugs. Biochem Biophys Res Commun. 2016; 469: 306-312.
19. Mate DM, Alcalde M. Laccase engineering: From rational design to directed evolution. Biotechnol Adv. 2015; 33: 25-40.
20. Pardo I, Camarero S. Laccase engineering by rational and evolutionary design. Cell Mol Life Sci. 2015; 72: 897-910.
21. Couto SR, Toca-Herrera JL. Laccase production at reactor scale by filamentous fungi. Biotechnol Adv. 2007; 25: 558-569.
22. Singh Arora D, Kumar Sharma R. Ligninolytic fungal laccases and their biotechnological applications. Appl Biochem Biotechnol. 2010; 160: 1760-1788.
23. Mansur M, Arias ME, Copa-Patiño JL, Flärdh M, González AE. The white-rot fungus Pleurotus ostreatus secretes laccase isozymes with different substrate specificities. Mycologia. 2003; 95: 1013-1020.
24. Kurniawati S, Nicell JA. Characterization of Trametes versicolor laccase for the transformation of aqueous phenol. Bioresour Technol. 2008; 99: 7825-7834.
25. Perry CR, Smith M, Britnell CH, Wood DA, Thurston CF. Identification of two laccase genes in the cultivated mushroom Agaricus bisporus. Microbiology. 1993; 139: 1209-1218.
26. Kilaru S, Hoegger PJ, Kües U. The laccase multi-gene family in Coprinopsis cinerea has seventeen different members that divide into two distinct subfamilies. Curr Genet. 2006; 50: 45-60.

27. Murugesan K, Nam IH, Kim YM, Chang YS. Decolorization of reactive dyes by a thermostable laccase produced by Ganoderma lucidum in solid state culture. Enzyme Microb Technol. 2007; 40: 1662-1672.
28. Banerjee UC, Vohra RM. Production of laccase by curvularia sp. Folia Microbiol. 1991; 36: 343-346.
29. Scherer M, Fischer R. Purification and characterization of laccase II of Aspergillus nidulans. Arch Microbiol. 1998; 170: 78-84.
30. Rodríguez A, Falcón MA, Carnicero A, Perestelo F, la Fuente GD, Trojanowski J. Laccase activities of Penicillium chrysogenum in relation to lignin degradation. Appl Microbiol Biotechnol. 1996; 45: 399-403.
31. Pawlik A, Ruminowicz-Stefaniuk M, Frąc M, Mazur A, Wielbo J, Janusz G. The wood decay fungus Cerrena unicolor adjusts its metabolism to grow on various types of wood and light conditions. PLoS One. 2019; 14: e0211744.
32. Zhang J, Sun L, Zhang H, Wang S, Zhang X, Geng A. A novel homodimer laccase from Cerrena unicolor BBP6: Purification, characterization, and potential in dye decolorization and denim bleaching. PLoS One. 2018; 13: e0202440.
33. Janusz G, Rogalski J, Szczodrak J. Increased production of laccase by Cerrena unicolor in submerged liquid cultures. World J Microbiol Biotechnol. 2007; 23: 1459-1464.
34. Rogalski J, Janusz G. Purification of extracellular laccase from Cerrena unicolor. Prep Biochem Biotechnol. 2010; 40: 242-255.
35. Deng K, Zeng J, Cheng G, Gao J, Sale KL, Simmons BA, et al. Rapid characterization of the activities of lignin-modifying enzymes based on nanostructure-initiator mass spectrometry (NIMS). Biotechnol Biofuels. 2018; 11: 266.
36. Ing N, Deng K, Chen Y, Aulitto M, Gin JW, Pham TLM, et al. A multiplexed nanostructure-initiator mass spectrometry (NIMS) assay for simultaneously detecting glycosyl hydrolase and lignin modifying enzyme activities. Sci Rep. 2021; 11: 11803.
37. Pham LTM, Deng K, Northen TR, Singer SW, Adams PD, Simmons BA, et al. Experimental and theoretical insights into the effects of pH on catalysis of bond-cleavage by the lignin peroxidase isozyme H8 from phanerochaete chrysosporium. Biotechnol Biofuels. 2021; 14: 108.
38. Elisashvili V, Kachlishvili E, Khardziani T, Agathos SN. Effect of aromatic compounds on the production of laccase and manganese peroxidase by white-rot basidiomycetes. J Ind Microbiol Biotechnol. 2010; 37: 1091-1096.
39. Waterhouse A, Bertoni M, Bienert S, Studer G, Tauriello G, Gumienny R, et al. SWISS-MODEL: Homology modelling of protein structures and complexes. Nucleic Acids Res. 2018; 46: W296-W303.
40. Olsson MHM, Søndergaard CR, Rostkowski M, Jensen JH. PROPKA3: Consistent treatment of internal and surface residues in empirical pKa predictions. J Chem Theory Comput. 2011; 7: 525-537.
41. Søndergaard CR, Olsson MH, Rostkowski M, Jensen JH. Improved treatment of ligands and coupling effects in empirical calculation and rationalization of pKa values. J Chem Theory Comput. 2011; 7: 2284-2295.
42. Kuriata A, Iglesias V, Pujols J, Kurcinski M, Kmiecik S, Ventura S. Aggrescan3D (A3D) 2.0: Prediction and engineering of protein solubility. Nucleic Acids Res. 2019; 47: W300-W307.

43. Brissos V, Chen Z, Martins LO. The kinetic role of carboxylate residues in the proximity of the trinuclear centre in the O_2 reactivity of CotA-laccase. Dalton Trans. 2012; 41: 6247-6255.
44. Phillips JC, Braun R, Wang W, Gumbart J, Tajkhorshid E, Villa E, et al. Scalable molecular dynamics with NAMD. J Comput Chem. 2005; 26: 1781-1802.
45. Huang J, Rauscher S, Nawrocki G, Ran T, Feig M, de Groot BL, et al. CHARMM36m: An improved force field for folded and intrinsically disordered proteins. Nat Methods. 2017; 14: 71-73.
46. Feller SE, Zhang Y, Pastor RW, Brooks BR. Constant pressure molecular dynamics simulation: The Langevin piston method. J Chem Phys. 1995; 103: 4613-4621.
47. de Leeuw SW, Perram JW, Smith ER, Rowlinson JS. Simulation of electrostatic systems in periodic boundary conditions. III. Further theory and applications. Proc R Soc Lond A. 1983; 388: 177-193.
48. Humphrey W, Dalke A, Schulten K. VMD: Visual molecular dynamics. J Mol Graph. 1996; 14: 33-38, 27-38.
49. Hartl FU, Bracher A, Hayer-Hartl M. Molecular chaperones in protein folding and proteostasis. Nature. 2011; 475: 324-332.
50. Stefani M, Dobson CM. Protein aggregation and aggregate toxicity: New insights into protein folding, misfolding diseases and biological evolution. J Mol Med. 2003; 81: 678-699.
51. Breydo L, Uversky VN. Role of metal ions in aggregation of intrinsically disordered proteins in neurodegenerative diseases. Metallomics. 2011; 3: 1163-1180.
52. Almagro Armenteros JJ, Tsirigos KD, Sønderby CK, Petersen TN, Winther O, Brunak S, et al. SignalP 5.0 improves signal peptide predictions using deep neural networks. Nat Biotechnol. 2019; 37: 420-423.
53. Chuang GY, Boyington JC, Joyce MG, Zhu J, Nabel GJ, Kwong PD, et al. Computational prediction of n-linked glycosylation incorporating structural properties and patterns. Bioinformatics. 2012; 28: 2249-2255.
54. Ben Younes S, Sayadi S. Purification and characterization of a novel trimeric and thermotolerant laccase produced from the ascomycete Scytalidium thermophilum strain. J Mol Catal B Enzym. 2011; 73: 35-42.
55. Hildén K, Hakala TK, Maijala P, Lundell TK, Hatakka A. Novel thermotolerant laccases produced by the white-rot fungus Physisporinus rivulosus. Appl Microbiol Biotechnol. 2007; 77: 301-309.
56. Campos PA, Levin LN, Wirth SA. Heterologous production, characterization and dye decolorization ability of a novel thermostable laccase isoenzyme from Trametes trogii BAFC 463. Process Biochem. 2016; 51: 895-903.
57. Spassov VZ, Yan L. A pH-dependent computational approach to the effect of mutations on protein stability. J Comput Chem. 2016; 37: 2573-2587.
58. Meuzelaar H, Vreede J, Woutersen S. Influence of Glu/Arg, Asp/Arg, and Glu/Lys salt bridges on α-helical stability and folding kinetics. Biophys J. 2016; 110: 2328-2341.
59. Baldrian P. Fungal laccases – occurrence and properties. FEMS Microbiol Rev. 2006; 30: 215-242.
60. Palmieri G, Cennamo G, Faraco V, Amoresano A, Sannia G, Giardina P. Atypical laccase isoenzymes from copper supplemented Pleurotus ostreatus cultures. Enzyme Microb Technol. 2003; 33: 220-230.

61. Frasconi M, Favero G, Boer H, Koivula A, Mazzei F. Kinetic and biochemical properties of high and low redox potential laccases from fungal and plant origin. Biochim Biophys Acta. 2010; 1804: 899-908.
62. Giardina P, Faraco V, Pezzella C, Piscitelli A, Vanhulle S, Sannia G. Laccases: A never-ending story. Cell Mol Life Sci. 2010; 67: 369-385.
63. Cañas AI, Camarero S. Laccases and their natural mediators: Biotechnological tools for sustainable eco-friendly processes. Biotechnol Adv. 2010; 28: 694-705.
64. d'Acunzo F, Galli C. First evidence of catalytic mediation by phenolic compounds in the laccase-induced oxidation of lignin models. Eur J Biochem. 2003; 270: 3634-3640.
65. Longe LF, Couvreur J, Leriche Grandchamp M, Garnier G, Allais F, Saito K. Importance of mediators for lignin degradation by fungal laccase. ACS Sustain Chem Eng. 2018; 6: 10097-10107.
66. Zeng J, Mills MJL, Simmons BA, Kent MS, Sale KL. Understanding factors controlling depolymerization and polymerization in catalytic degradation of β-ether linked model lignin compounds by versatile peroxidase. Green Chem. 2017; 19: 2145-2154.
67. Camarero S, Ibarra D, Martínez MJ, Martínez AT. Lignin-derived compounds as efficient laccase mediators for decolorization of different types of recalcitrant dyes. Appl Environ Microbiol. 2005; 71: 1775-1784.
68. Nousiainen P, Maijala P, Hatakka A, Martínez AT, Sipilä J. Syringyl-type simple plant phenolics as mediating oxidants in laccase catalyzed degradation of lignocellulosic materials: Model compound studies 10th EWLP, Stockholm, Sweden, August 25–28, 2008. Holzforschung. 2009; 63: 699-704.
69. Chen X, Ouyang X, Li J, Zhao YL. Natural syringyl mediators accelerate laccase-catalyzed β-O-4 cleavage and Cα-oxidation of a guaiacyl model substrate via an aggregation mechanism. ACS Omega. 2021; 6: 22578-22588.
70. Shleev S, Jarosz-Wilkolazka A, Khalunina A, Morozova O, Yaropolov A, Ruzgas T, et al. Direct electron transfer reactions of laccases from different origins on carbon electrodes. Bioelectrochemistry. 2005; 67: 115-124.
71. Michniewicz A, Ullrich R, Ledakowicz S, Hofrichter M. The white-rot fungus Cerrena unicolor strain 137 produces two laccase isoforms with different physico-chemical and catalytic properties. Appl Microbiol Biotechnol. 2006; 69: 682-688.
72. Haibo Z, Yinglong Z, Feng H, Peiji G, Jiachuan C. Purification and characterization of a thermostable laccase with unique oxidative characteristics from Trametes hirsuta. Biotechnol Lett. 2009; 31: 837-843.
73. Autore F, Del Vecchio C, Fraternali F, Giardina P, Sannia G, Faraco V. Molecular determinants of peculiar properties of a Pleurotus ostreatus laccase: Analysis by site-directed mutagenesis. Enzyme Microb Technol. 2009; 45: 507-513.
74. Vasdev K, Dhawan S, Kapoor RK, Kuhad RC. Biochemical characterization and molecular evidence of a laccase from the bird's nest fungus Cyathus bulleri. Fungal Genet Biol. 2005; 42: 684-693.
75. Hämäläinen V, Grönroos T, Suonpää A, Heikkilä MW, Romein B, Ihalainen P, et al. Enzymatic processes to unlock the lignin value. Front Bioeng Biotechnol. 2018; 6: 20.

76. Yin Q, Zhou G, Peng C, Zhang Y, Kües U, Liu J, et al. The first fungal laccase with an alkaline pH optimum obtained by directed evolution and its application in indigo dye decolorization. AMB Express. 2019; 9: 151.
77. Novoa C, Dhoke GV, Mate DM, Martínez R, Haarmann T, Schreiter M, et al. Knowvolution of a fungal laccase toward alkaline pH. Chembiochem. 2019; 20: 1458-1466.
78. Xu F. Effects of redox potential and hydroxide inhibition on the pH activity profile of fungal laccases. J Biol Chem. 1997; 272: 924-928.